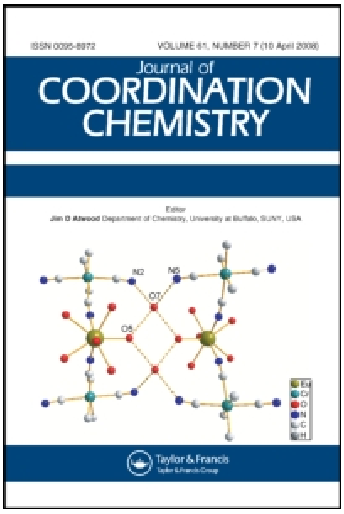

Journal of Coordination Chemistry
Publication details, including instructions for authors and subscription information:
http://www.informaworld.com/smpp/title~content=t713455674

Syntheses, structures and properties of three neutral bisupporting heteropolyoxometalates

Hong-Bo Liu[ab]; Yu Sun[a]; Ya-Guang Chen[a]; Fan-Xia Meng[a]; Dong-Mei Shi[a]
[a] Key Laboratory of Polyoxometalates Science of Ministry of Education, College of Chemistry, Northeast Normal University, Changchun 130024, P. R. China [b] Department of Pharmaceutics, Changchun Medical College, Changchun 130031, P.R. China

To cite this Article Liu, Hong-Bo , Sun, Yu , Chen, Ya-Guang , Meng, Fan-Xia and Shi, Dong-Mei(2008) 'Syntheses, structures and properties of three neutral bisupporting heteropolyoxometalates', Journal of Coordination Chemistry, 61: 19, 3102 — 3109

To link to this Article: DOI: 10.1080/00958970802001780

URL: http://dx.doi.org/10.1080/00958970802001780

Journal of Coordination Chemistry
Vol. 61, No. 19, 10 October 2008, 3102–3109

Syntheses, structures and properties of three neutral bisupporting heteropolyoxometalates

HONG-BO LIU[†][‡], YU SUN[†], YA-GUANG CHEN*[†],
FAN-XIA MENG[†] and DONG-MEI SHI[†]

[†]Key Laboratory of Polyoxometalates Science of Ministry of Education, College of Chemistry, Northeast Normal University, Changchun 130024, P. R. China
[‡]Department of Pharmaceutics, Changchun Medical College, Changchun 130031, P.R. China

(*Received 18 September 2007; in final form 5 December 2007*)

Three neutral polyoxometalates $[PVW_{11}O_{40}\{M(phen)_2H_2O\}_2]\cdot 3H_2O$ (phen = 1,10′-phenanthroline, M=Co **1**, Zn **2**, Ni **3**) are composed of water and the neutral Keggin-type polyoxometallate covalently linking a pair of transition metal complex fragments on opposite sides. The transition metal lies in the center of a distorted octahedron. Multi hydrogen-bonding interactions between coordinated waters of neutral polyoxometalate molecules and terminal oxygen atoms of Keggin units and between bridging oxygens of Keggin units and lattice water create a two dimensional layer and between the layers there exist van der Waals forces. The framework of the neutral molecule begins to decompose at ca 500°C. Compound **1** exhibits a weak antiferromagnetic interaction in the 2–300 K range.

Keywords: Hydrothermal synthesis; Thermal analysis; Crystal structure; Neutral polyoxotungstate; Organo-inorganic hybrids

1. Introduction

Polyoxometalates (POMs) have potential applications in catalysis, sorption, medicine, electrical conductivity, magnetism and photochemistry as well as the intriguing topological features [1]. Recent progress in polyoxotungstate chemistry is the decoration of polyoxotungstate with various organic groups and/or transition metal complexes to produce polyoxoanion-supporting inorganic-organic hybrid materials. Introduction of transition metal-ligand units not only enrich the polyoxotungstate framework but also ameliorate their electronic and magnetic properties [2–7]. However, heteropolyoxoanion-supporting hybrid solids have been less reported than isopolyoxoanion-supporting hybrid solids due to the deficient charge density on the surface oxygen atoms of heteropolyoxoanions. In general, two strategies may be exploited to increase the surface charge density and activate the surface oxygen atoms of heteropolyoxoanion [8]: (a) reduce the metal centers from high oxidation state to low

---

*Corresponding author. Email: chenyg146@nenu.edu.cn

Journal of Coordination Chemistry
ISSN 0095-8972 print/ISSN 1029-0389 online
DOI: 10.1080/00958970802001780

oxidation state by introducing strong reducing reagents, from W(VI) to W(V), for instance, $[PW^{VI}{}_{10}W^{V}{}_{2}O_{40}Ni(2,2'\text{-bipy})_2(H_2O)]^{3-}$ [9] and $[PMo^{VI}{}_{9}Mo^{V}{}_{3}O_{40}\{Ni(phen)\}_2]^{2-}$ [10]; or (b) replace high oxidation state metal centers by another low-valence metal, for example, from W(VI) to V(V) such as $[PW_9V_3O_{40}\{Ag(2,2'\text{-bipy})\}_2\{Ag_2(2,2'\text{-bipy})_3\}_2]$ [11]. Following the second strategy, the title compounds are separated under hydrothermal conditions, continuing our previous work [12–14].

2. Experimental

2.1. *General procedures*

All chemicals purchased were of reagent grade from commercial sources and used without further purification. Distilled water is used in the reactions. Elemental analyses (C, H and N) were performed on a Perkin-Elmer 2400 CHN elemental analyzer. W, V, Co, Ni and Zn were determined by a Leaman inductively coupled plasma (ICP) spectrometer. IR spectra were recorded in the range 400–4000 cm^{-1} on a Magna-560 FT/IR spectrophotometer using KBr. TG analyses were performed on a Perkin-Elmer TGA7 instrument in flowing N_2 with a heating rate of 10°C min^{-1}. Magnetism has been examined on crystalline samples using a Quantum Design MPMS-5SQUID magnetometer in the range of 2–300 K.

2.2. *Synthesis*

2.2.1. $[PVW_{11}O_{40}\{Co(phen)_2H_2O\}_2]\cdot 3H_2O$ (1). The best crystals of **1** were prepared from a reaction mixture of $Na_2WO_4\cdot 2H_2O$ (1.0 g), $CoCl_2\cdot 6H_2O$ (0.23 g), phen (0.34 g), NH_4VO_3 (0.3 g) and 0.2 mL 85% H_3PO_4 in 15 mL water. The starting mixture was adjusted to pH = 2.7 by addition of 4 mol L^{-1} aqueous HCl, and then transferred into a 25 mL Teflon–lined autoclave at 160°C for 120 h. Then the autoclave was cooled at 10°C h^{-1} to room temperature. The resulting dark-red block crystals were filtered off, washed with distilled water, and dried at ambient temperature (yield: ca 60% based on W). Elemental analysis of the crystals is consistent with the stoichiometry of **1**. Anal. Calcd (%) for $C_{48}H_{32}Co_2N_8O_{45}PVW_{11}$: C, 15.7; H, 0.9; N, 3.1; Co, 3.31; V, 1.4; W, 55.1. Found (%): C, 15.4; H, 0.85; N, 2.95; Co, 3.27; V, 1.46; W, 55.3.

2.2.2. $[PVW_{11}O_{40}\{Zn(phen)_2H_2O\}_2]\cdot 3H_2O$ (2). The best crystals of **2** were prepared from a reaction mixture of $Na_2WO_4\cdot 2H_2O$ (1.0 g), NH_4VO_3 (0.3 g), $Zn(CH_3COO)_2\cdot 2H_2O$ (0.39 g), phen (0.34 g), and 0.2 mL 85% H_3PO_4 in 15 mL water. The starting mixture was adjusted to pH = 4.3 by addition of 4 mol·L^{-1} aqueous HCl, and then transferred to a 25 mL Teflon–lined autoclave at 160°C for 120 h. The autoclave was cooled at 10°C·h^{-1} to room temperature and the resulting orange-red block crystals were filtered off, washed with distilled water, and dried at ambient temperature (yield: ca 40% based on W). Elemental analyses of the crystals are consistent with the stoichiometry. Anal. Calcd (%) for $C_{48}H_{32}N_8O_{45}PVW_{11}Zn_2$: C, 15.6; H, 0.9; N, 3.0; V, 1.4; W, 55.0; Zn, 3.6. Found (%): C, 15.4; H, 0.8; N, 2.95; V, 1.54; W, 55.3; Zn, 3.68.

2.2.3. [$PVW_{11}O_{40}$\{Ni(phen)$_2H_2O$\}$_2$] · $3H_2O$ (3). The best crystals of **3** were prepared from reaction of $Na_2WO_4 \cdot 2H_2O$ (1.0 g), $NiSO_4 \cdot 6H_2O$ (0.32 g), NH_4VO_3 (0.3 g), phen (0.34 g) and 0.2 mL 85% H_3PO_4 in 15 mL water. The mixture was adjusted to pH = 4.9 by addition of 4 mol L^{-1} aqueous HCl and transferred into a 25 mL Teflon–lined autoclave and reacted at 160°C for 96 h. The autoclave was cooled at 10°C h^{-1} to room temperature. The resulting orange-yellow block crystals were filtered off, washed with distilled water, and dried at ambient temperature (yield: ca 40% based on W). Elemental analyses of the crystals are consistent with the stoichiometry of **3**. Anal. Calcd (%) for $C_{48}H_{32}N_8Ni_2O_{45}PVW_{11}$: C, 15.7; H, 0.9; N, 3.1; Ni, 3.41; V, 1.4; W, 55.2. Found (%): C, 15.6; H, 0.83; N, 2.98; Ni, 3.35; V, 1.48; W, 55.3.

2.3. *X-ray crystallography*

Single crystals were carefully selected under a polarizing microscope and glued at the tip of a thin glass fiber with cyanoacrylate (superglue) adhesive. Data were collected on a Smart Apex CCD diffractometer (for **1** and **2**) a Rigaku IIIA IP diffractometer (for **3**) at 293 K using graphite-monochromated Mo-K_α radiation ($\lambda = 0.71073$ Å) and omega scans technique and an empirical absorption correction was applied. The structures were solved by the direct method and refined by full-matrix least-squares on F^2 using SHELXL 97 software [15]. All non-hydrogen atoms were easily located from subsequent Fourier difference maps and refined anisotropically. Hydrogen atoms were added according to theoretical models. A summary of the crystallographic data and structural refinements for these compounds is provided in table 1. The CCDC numbers are 602002 for **1**, 606060 for **2** and 611757 for **3**.

3. Results and discussion

3.1. *Formation of the compounds*

From simple oxometalates, Na_2WO_4, NH_4VO_3, and H_3PO_4, **1**, **2** and **3** were formed under hydrothermal conditions with different transition metals. They all contain monosubstituted Keggin anion, differing from that reported [13] in which the pre-synthetic saturated Keggin anion was the starting material. Although the starting reaction solutions have different pH values, the polyoxoanions of the products are identical. That is, pH values from 2.7 to 4.9 are suitable for formation of the monosubstituted Keggin anion $PW_{11}VO_{40}^{4-}$ but are required for surface decoration of the anion with different metal coordination fragments.

3.2. *Structure descriptions*

Compounds **1**, **2**, and **3** crystallize in the same crystal system and space group (table 1) and their cell parameters are almost identical; **1** is taken as an example for their structural discussion. Compound **1** comprises a neutral bisupporting heteropolyoxometalate $[PW_{11}VO_{40}\{Co(phen)_2(H_2O)\}_2]$ (figure 1) and three lattice water molecules. The neutral molecule $[PW_{11}VO_{40}\{Co(phen)_2(H_2O)\}_2]$ consists of the mixed tungsten-vanadium polyoxoanion $[PW_{11}VO_{40}]^{4-}$ and two cobalt(II) complex fragments $[Co(phen)_2(H_2O)]^{2+}$ covalently linked on opposite sites. The heteropolyanion $[PW_{11}VO_{40}]^{4-}$ has the well-known α-Keggin-type structure, formed from 12 MO_6 octahedra (W and V are of site occupancy disorder, each $M = 11/12W + 1/12V$) and one PO_4 tetrahedron. The PO_4 tetrahedron (atoms O_a) is surrounded by four corner-sharing M_3O_{13} units formed by three edge-sharing MO_6 octahedra (corner-sharing O atoms between M_3O_{13} units are denoted O_b, edge-sharing O atoms within M_3O_{13} units are denoted O_c and unshared terminal O atoms are denoted O_t). The central P is located at the inversion center and surrounded by a cube of eight oxygen atoms, with each oxygen site half-occupied and with P–O distances of 1.504(14)–1.559(14) Å, the anion is of orientational disorder. All tungsten and vanadium atoms are distorted $\{MO_6\}$ octahedra with different M–O distances: M–O_t 1.633(9)–1.696(7), M–$O_{b/c}$ 1.859(10)–1.928(10),

Table 1. Crystallographic and refinement data of the compounds.

Compound	**1**	**2**	**3**
Empirical formula	$C_{48}H_{36}N_8Co_2O_{45}PVW_{11}$	$C_{48}H_{36}N_8O_{45}PVW_{11}Zn$	$C_{48}H_{36}N_8Ni_2O_{45}PVW_{11}$
Formula weight	3666.97	3679.87	3666.49
Temperature (K)	293		
Wavelength (Å)	0.71073		
Crystal system, space group	Triclinic, *P*-1		
Unit cell dimensions (Å, °)			
a	10.965(5)	10.9448(4)	10.973(2)
b	13.330(5)	13.3299(5)	13.307(3)
c	13.645(5)	13.6522(5)	13.602(3)
α	69.257(5)	69.1080(10)	69.30(3)
β	71.394(5)	71.3230(10)	71.18(3)
γ	78.395(5)	78.3400(11)	78.14(3)
Volume (Å^3)	1758.9 (12)	1754.10(11)	1749.0(6)
Z, D_{Calcd} (Mg m^{-3})	1, 3.458	1, 3.606	1, 3.596
Absorption coefficient (mm^{-1})	18.615	18.945	20.294
F(000)	1642	1699	1693
Crystal size (mm^3)	0.19 × 0.16 × 0.15	0.16 × 0.15 × 0.14	0.19 × 0.16 × 0.14
θ range for data collection (°)	1.64 to 28.48	1.64 to 28.68	3.15 to 26.00
Limiting indices	$-14 \leq h \leq 14$ $-17 \leq k \leq 15$ $-16 \leq l \leq 17$	$-13 \leq h \leq 14$ $-11 \leq h \leq 17$ $-18 \leq h \leq 18$	$-13 \leq h \leq 13$, $-15 \leq k \leq 16$, $-16 \leq l \leq 16$
Reflections collected/unique $R_{(\text{int})}$	10917/7830 0.0244	10846/7848 0.0214	15145/6852 0.0845
Completeness(%)	87.9(28.48°)		99.5(26.00°)
Absorption correction	Empirical		
Max. and min. transmission	0.061, 0.041	0.031, 0.017	0.061, 0.041
Refinement method	Full-matrix least squares on F^2		
Data/restraints/parameters	7830/0/545	7848/0/540	6852/0/545
Goodness-of-fit on F^2	1.068	1.033	1.054
R_1, wR_2 [$I > 2\sigma(I)$]	0.0438, 0.1230	0.0474, 0.1388	0.0604, 0.1340
R indices (all data) R_1, wR_2	0.0496, 0.1266	0.0561, 0.1495	0.1042, 0.1498
Extinction coefficient	0.00080(8)	0.000618(8)	0.00036(9)
Largest diff. peak and hole (e Å^{-3})	2.72, −4.57	2.529, −4.826	2.38, −3.24

M–Oa 2.418(14)–2.498(14) Å, and their mean values are 1.663, 1.893 and 2.460 Å, respectively, consistent with those in the literature [16, 17].

The $[PW_{11}VO_{40}]^{4-}$ anion is a bidentate ligand, covalently bonding to two $[Co(phen)_2(H_2O)]^{2+}$ fragments through opposite terminal oxygen atoms, forming a bisupporting polyoxometalate. This is unlike the compound previously reported [13] in which the complex fragments link through one terminal oxygen atom and one bridging oxygen atom on non-opposite sites. The bonding of two $[Co(phen)_2(H_2O)]^{2+}$ fragments gives a neutral molecule. The Co is coordinated by four nitrogen atoms from two 1,10-phenanthrolines with Co–N distances of 2.114(9)–2.144(9) Å and N–Co–N angles of 79.0(4)–172.9(6)°, one oxygen from the $[PW_{11}VO_{40}]^{4-}$ anion and a water with Co–O distances of 2.113(8) and 2.114(8) Å to finish its distorted octahedron.

Coordination and lattice water molecules participate in multi hydrogen bonds with surface oxygens of the Keggin unit. As shown in figure 2, each neutral molecule utilizes its coordination water (O20W) in the complex fragments to form two hydrogen bonds with surface oxygen atoms (O2) of the Keggin units of the two adjacent neutral molecules; in turn, two adjacent neutral molecules utilize their coordination waters to form two hydrogen bonds with surface oxygens of the Keggin unit. As a result of these hydrogen bond interactions, a one dimensional chain forms and lattice waters link two neutral molecules of adjacent chains through two hydrogen bonds (O22W–O8) forming a layer in the *ac* plane. Van der Waals forces and weak hydrogen bonds

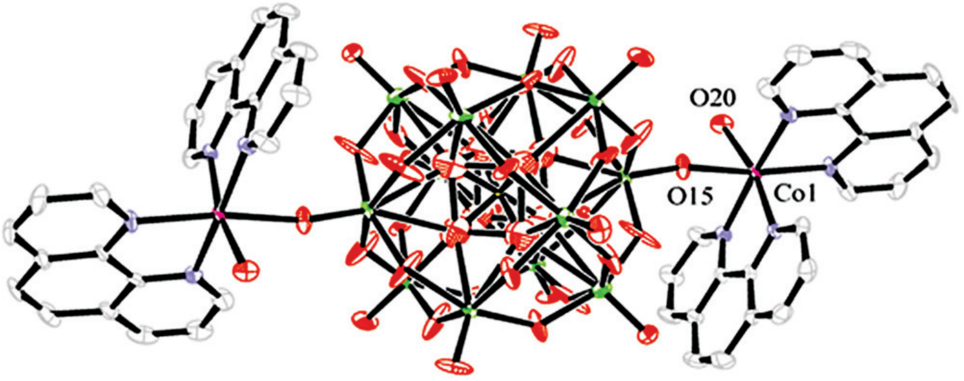

Figure 1. ORTEP drawing of $[\{Co(phen)_2(H_2O)\}_2PW_{11}VO_{40}] \cdot 3H_2O$ depicted at 30% probability level, only some atoms are labeled and all H atoms are omitted for clarity.

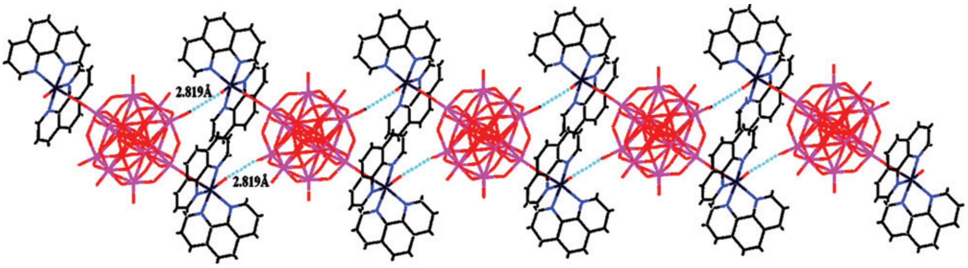

Figure 2. View of the hydrogen bonds between the neutral molecules viewed along the *a*-axis.

(between CH of phen ring and surface oxygen atoms, C20 $\cdots$ O5 3.384 and CH $\cdots$ O 2.684) link the layers (figure 3).

Compounds **2** and **3** are isostructural with **1** containing transition metal complex fragments in distorted octahedral coordination environment; the geometric data are listed in table 2. The linkages between molecules and their arrangement are almost identical with **1**.

3.3. *TG analyses*

The TG curve (figure S1) of **1** shows two weight loss stages, giving a total loss of 21.52% in the range 35–729°C, which approximately agrees with the calculated value of 22.08%. The weight loss (2.39%) of the first step (35–220.9°C) corresponds to the release of lattice and coordinated water molecules (Calcd 2.45%), and the weight loss (19.70%) of the second step (354–730.1°C) is attributed to the loss of phen molecules (Calcd 19.63%). The framework of the neutral molecule began to decompose at ca 500°C. Compounds **2** and **3** have very similar TG curves and the corresponding weight losses are 2.41% (2.44%) in 35–217°C and 19.0% (19.56%) in 350.9–728.2°C for **2**

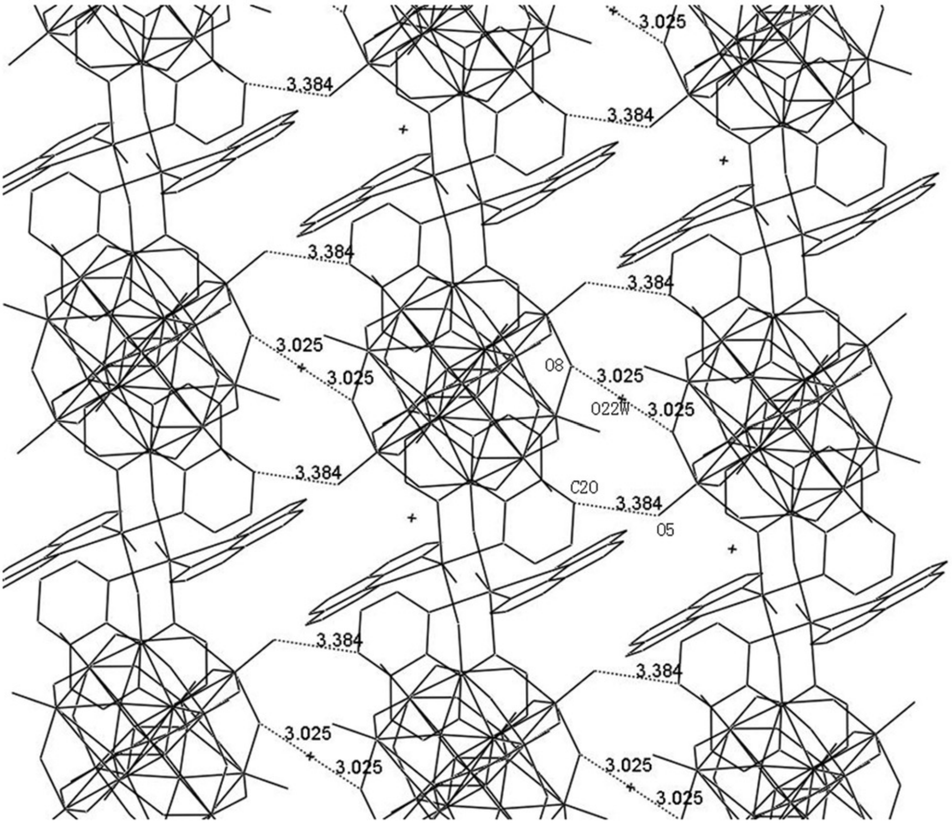

Figure 3. The packing arrangement of **1** viewed along the *c*-axis.

(figure S2); 2.40% (Calcd 2.45%) in 35–219°C and 19.12% (Calcd 19.64%) in 347–729°C for **3** (figure S3).

3.4. *Magnetic properties*

The variable-temperature magnetic behavior at fixed field strength of 1000 Oe for **1** is shown in figure 4 in the form of $\chi_m T$ *versus*. T and $1/\chi_m$ *versus*. T curves. The $\chi_m T$ value

Table 2. Selected bond lengths (Å) and angles (°).

1		2		3	
Co1–O20	2.114(8)	Zn1–N3	2.111(11)	Ni1–N5	2.059(14)
Co1–O15	2.113(8)	Zn1–O5	2.119(9)	Ni1–N8	2.069(18)
Co1–N3	2.114(9)	Zn1–N1	2.140(10)	Ni1–O90	2.079(16)
Co1–N2	2.138(9)	Zn1–N4	2.150(10)	Ni1–N10	2.085(17)
Co1–N4	2.143(9)	Zn1–N2	2.152(10)	Ni(1)–N(4)	2.093(15)
Co1–N1	2.144(9)	Zn1–O1	2.207(8)	Ni(1)–O(18)	2.106(12)
O20–Co1–O15	86.2(3)	N3–Zn1–O5	94.9(4)	O90–Ni1–O18	86.3(6)
O20–Co1–N3	93.8(4)	N3–Zn1–N1	105.8(4)	N5–Ni1–O90	94.2(6)
O15–Co1–N3	169.3(4)	O5–Zn1–N1	92.9(4)	N8–Ni1–O90	170.3(6)
O20–Co1–N2	93.5(3)	N3–Zn1–N4	79.0(4)	O90–Ni1–N10	92.2(7)
O15–Co1–N2	87.4(3)	O5–Zn1–N4	94.7(4)	N5–Ni1–O18	87.2(6)
N3–Co1–N2	103.2(4)	N1–Zn1–N4	170.7(4)	N5–Ni1–N4	102.3(6)
O20–Co1–N4	93.9(3)	N3–Zn1–N2	98.3(4)	O90–Ni1–N4	91.4(7)
O15–Co1–N4	90.5(3)	O5–Zn1–N2	165.7(4)	N10–Ni1–O18	90.1(6)
N3–Co1–N4	78.8(4)	N1–Zn1–N2	78.2(4)	N5–Ni1–N8	79.0(7)
N2–Co1–N4	172.1(4)	N4–Zn1–N2	93.4(4)	N5–Ni1–N10	172.9(6)
O20–Co1–N1	168.4(3)	N3–Zn1–O1	167.6(4)	N4–Ni1–O18	170.3(6)
O15–Co1–N1	85.4(3)	O5–Zn1–O1	84.3(3)	N8–Ni1–O18	86.6(6)
N3–Co1–N1	95.9(4)	N1–Zn1–O1	86.6(4)	N8–Ni1–N4	96.8(7)
N2–Co1–N1	78.1(4)	N4–Zn1–O1	88.7(4)	N10–Ni1–N4	80.7(6)
N4–Co1–N1	94.1(4)	N2–Zn1–O1	84.0(4)	N8–Ni1–N10	94.3(7)

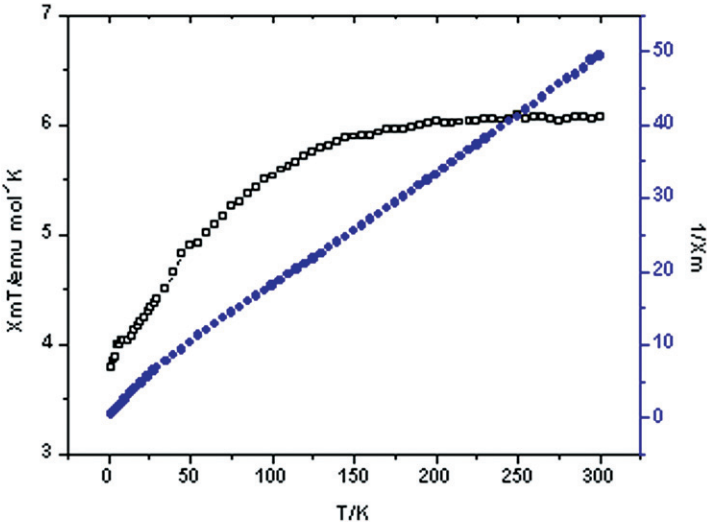

Figure 4. Temperature dependence of $1/\chi_m$ and $\chi_m T$ for **1**.

decreases with lowering temperature, reaching 3.80 emu K mol^{-1} at 2 K. This magnetism is typical of antiferromagnetic interactions in the 2–300 K temperature range. According to the results of crystal structure analysis, the weak antiferromagnetic interactions must be through π–π interactions of phen rings due to the separation of two paramagnetic centers by the antimagnetic polyoxoanion and no reduced metal atoms. It can be seen from $1/\chi_m$-T curve that the magnetic susceptibility obeys the Curie-Weiss law in the range 2–300 K with C = 6.6 emu K mol^{-1} and $\theta = -20$ K. At 300 K, the effective magnetic moment (μ_{eff}) determined from the equation $\mu_{eff} = 2.828(\chi_m T)^{1/2}$ is 7.06 μ_B, higher than expected for two high-spin octahedral Co(II) ions (6.901 μ_B, supposed g = 2.52), suggesting orbital contributions to the effective magnetic moment ($\mu_{S+L} = 7.72$, supporting $g = 2.52$, approaching the experimental value). From the structural similarity, **3** should have same magnetic interaction behavior; very similar magnetic behavior was observed [12] for a compound with similar bisupporting structure.

Acknowledgement

This work was supported by the Analysis and Testing Foundation of Northeast Normal University.

References

[1] M.T. Pope, A. Müller. *Polyoxometalate Chemistry*, Dordrecht, Kluwer (2001).
[2] P.J. Hagrman, D. Hagrman, J. Zubieta. *Angew. Chem., Int. Ed. Engl.*, **38**, 2638 (1999).
[3] U. Kortz, M.G. Savelieff, F.Y. Abou Ghali, L.M. Khalil, S.A. Maalouf, D.L. Sinno. *Angew. Chem., Int. Ed.*, **41**, 4070 (2002).
[4] U. Kortz, J. Vaissermann, R. Thouvenot, P. Gouzerh. *Inorg. Chem.*, **42**, 1135 (2003).
[5] A.J. Stein, S.W. Keller, T.E. Mallouk. *Science*, **259**, 1558 (1993).
[6] M. Yuan, Y.G. Li, E.B. Wang, Y. Lu, C.W. Hu, N.H. Hu, H.Q. Jia. *J. Chem. Soc., Dalton Trans.*, 2916 (2002).
[7] P.J. Zapf, C.J. Warren, R.C. Haushalter, J. Zubieta. *Chem. Commun.*, 1543 (1997).
[8] P. Gouzerh, A. Proust. *Chem. Rev.*, **98**, 77 (1998).
[9] Y. Xu, J.Q. Xu, K.L. Zhang, Y. Zhang, X.Z. You. *Chem. Commun.*, 153 (2000).
[10] M. Yuan, Y.G. Li, E.B. Wang, C.G. Tian, L. Wang, C.W. Hu, N.H. Hu, H.Q. Jia. *Inorg. Chem.*, **42**, 3670 (2003).
[11] G.Y. Luan, Y.G.. Li, S.T. Wang, E.B. Wang, Z.B. Han, C.W. Hu, N.H. Hu, H.Q. Jia. *J. Chem. Soc., Dalton Trans.*, 233 (2003).
[12] K. Liu, F.X. Meng, Y.G. Chen. *Transition Met. Chem.*, **32**, 350 (2007).
[13] F.X. Meng, Y. Sun, K. Liu, F.X. Ma, Y.G. Chen. *J. Coord. Chem.*, **60**, 401 (2007).
[14] K. Liu, F.X. Meng, F.X. Ma, Y.G. Chen. *Chem. Res. Chinese U.*, **23**, 391 (2007).
[15] (a) G.M. Sheldrick. *SHELXS 97, Program for Crystal Structure Solution*, University of Göttingen Germany (1997); (b) G.M. Sheldrick. *SHELXL 97, Program for Crystal Structure Refinement*, University of Göttingen Germany (1997).
[16] T.H. Evans, M.T. Pope. *Inorg. Chem.*, **23**, 501 (1984).
[17] D. Attanasio, M. Bonamico, V. Fares, P. Imperatori, L. Suber. *J. Chem. Soc., Dalton Trans.*, 3221 (1990).